MVA '92 IAPR Workshop on Machine Vision Applications Dec. 7-9,1992, Tokyo

Under the sun light. From physics to image processing

COLLIN.B * ZAVIDOVIQUE.B **

* ETCA/CREA/SP 16 bis av. Prieur de la Côte d'Or 94114 ARCUEIL CEDEX, FRANCE
tel: (33) 1 4231 9863 E-mail : yak@etca.fr
** IEF-ETCA Université de Paris-Sud Orsay, FRANCE tel: (33) 1 4231 9719 E-mail : zavido@etca.fr

ABSTRACT

The observation of the sun dates back to antiquity. Strong assumptions lead the astrophysical community to say that long-range climatic trends commonly observed on the earth surface are due to the solar activity. Then it is worth studying at least the convective zone just below the surface which is observable, to analyze the motion of the matter. Making one's way into the sun is thus releavant, we first describe briefly the solar convection as well as magnetic signs appearing at the surface.

Analysis of solar images and surveillance of the solar activity being in great need of computerization, image processing appeared a natural response to the astrophysicists. Conversely computer scientists understood very soon that for sufficient accuracy, processes need to be designed in accordance with the very physical phenomena. Embedding the solar knowledge along a hierarchical network allowed to optimize the algorithms, for instance using sharper criteria on less regions during segmentation. The cooperation between physics and image processing was fruitful, as proved a complete absence of false alarm, as well as the detection accuracy, not to forget a relative simplicity of methods. In the second part we describe the elaboration of a semantic network (interaction of structures within layers) and we outline proposed images processing solutions.

The third part is devoted to the complete segmentation line, from raw data to automatic structure tracking. Original pictures are corrected, accounting for terrestrial moves. Then , all releavant so called "inhomogeneous" zones are extracted through autoadaptative thresholdings on a textural index. Here is where physics matters first as this index results from the physical analysis, excluding any visual evaluation. Regions are validated and classified thanks to luminosity, size and position/form criteria.

The fourth part describes the tracking, through a prediction/verification scheme. We discuss how structures are represented as sets of lines, following again astrophysicists' knowledge. We show that the use of dynamic programming on multi scale edge data can perform both region tracking and point to point matching between two associated regions.

In the last part different steps of the algorithms are illustrated. We show several enlargements of the detected regions which highlight the algorithm precision, before to conclude on the new possibilities for solar astrophysicists to ascertain some hypotheses that should lead to historical findings.

1 THE SUN, A VARIABLE STAR

The sun has been observed and studied for a long time. The famous black sunspots have been tracked since first age Chineese astrophysicists began to study them in Antiquity. The first observation was the variability of their number. Then, with the new coming technologies, their movements were quantified. They were proved to fit a differrential rotation law, which means that the sunspots velocities obey the following formula:

$$\Omega = \alpha \sin^2 \lambda + \beta$$

where

Ω is the rotation in degree/day

λ the latitude

α β are experimental constants

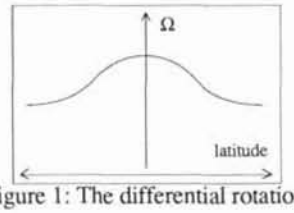

Figure 1: The differential rotation

Thus, they move faster around the equatorial regions than near the north and south poles (*see figure1*).Astrophysicists found that, beyond these variabilities, was hidden the motion of a badly known convective zone.

They began to get interested in the way matter flows from the inner sun to the surface, first of all to understand the star but also because its complex pulsations [1]were proved to interact with long range terrestrial climatic trends.

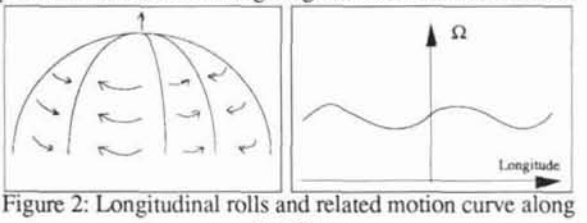

Figure 2: Longitudinal rolls and related motion curve along equator

The convective zone is the place in the sun where energy is carried by the matter flow. Two theories depict the way the carrying is supposed to be organized. One relies on the existence of longitudinal rolls and leads to a periodic surface motion curve as shown in *figure 2*. The other is built on azimuthal rolls [2]. In that case we will distinguish two kinds of roll pairs.One is called "downdraft"; it is composed of two converging rolls that carry matter from surface to depth so enhancing the differential nature of the rotation law.

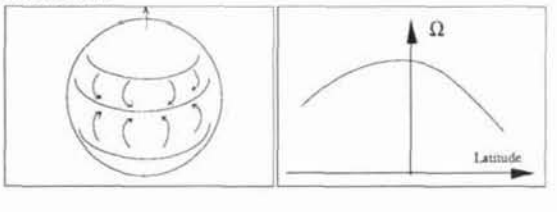

Figure 3: Downdraft and rotation law

The other is called "updraft" and has opposite effects on the rotation law.

Nowadays, technologies do not allow a straight analysis of the convective zone. But its organization is known to influence deeply the superficial motion, hence our goal : the detection of the surface movement.

Astrophysicists working with solar images of the chromosphere (wing CaII 3933A called Hα radiation) often deal with two different magnetical structures observable for this wave length.*Faculas* come in the form of bright spots. They frame the emergence of magnetical field tubes under the effect of magnetical pressure as depicted in *figure 4*. The top and bottom of this set of tubes (north and south polarities) are seen as small dark spots, studied for years, and much better known as the sunspots.*Filaments* appear as threadlike dark regions. They are, to some extent, leaves of plasma, suspended upon the surface thanks to magnetic forces. In consequence, they are laid across magnetical lines as shown in *figure 4*.

Because of complex entropy transfers between their inner and their outer parts, faculas, appear bright. Conversely, filaments absorb the incident radiation and look dark.

The search for the surface motion has always gone through detecting and tracking sunspots. There are two reasons:

• historically, sunspots have been studied for a long time as they are visible to the naked eye. So there are a lot of data, starting from Antiquity to nowadays.

• sunspots are easier to detect than filaments or faculas. They can be represented as small dots and thus the calculation of the movement shows sufficient accuracy as no internal deformations occur to false measures.

But day after day, since 1917, three pictures of the solar surface (3 different frequencies KIV, KIII and Hα) have been taken by Observatories in the world, and this amount of data, combined with a crucial need for increased accuracy, has naturally led to human processing first, then interactive and now automatic image processing: surveillance and tracking will be rely here on both filaments and faculas.

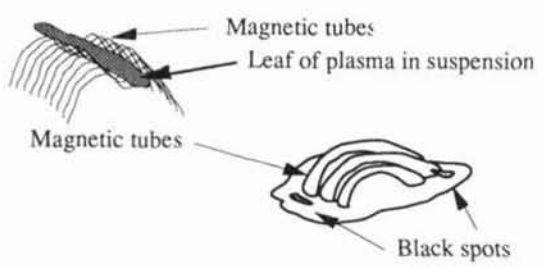

figure 4: Schematic representation of a filament and a facula

2 DERIVING PROCESSES FROM PHYSICAL KNOWLEDGE

As we got some a priori knowledge coming from the physical observations, we will detail how the design of the application dedicated algorithms is bound to this knowledge. Indeed such models, derived from physics, are as relevant as any other type of model (geometriy, structure...) in so far as they found automatic preseting of variables like thresholds. Exactly like geometric models, in 3D reconstruction help derive a distance or any equilibrium state from the sensed silhouette, physics give ideas about weight or surface-state. But in our case an additional benefit from this knowledge is the very choice of variables: for instance we show how quite elementary physics understanding leads to favour texture, giving up with edges, even if common sense intuition would go against and be wrong.

The aim of the application is to extract sun's surface dynamics as it is of first interest for astrophysicists. The raw data come from a spectroheliograph sited on earth (at Meudon's Observatory). Thus the luminosity of the images strongly depends on the atmosphere transparency and to a lesser extent on the transfer function of the spectroheliograph. Inverting atmosphere transfer function would be impossible and in any case remains a physicist's work. As for image processing, motion detection inside from image sequence can be separated in two major class as:

• optical flow, that uses differential methods and based upon a strong luminosity invariance constraint .

• segmentation and then region inter image tracking.

Thus, using raw data leads naturally (or "physically") to the second choice, all the more since there are pertinent areas on the sun surface that can be tracked despite their uneven luminosity. Our design will be separated in two parts, first the segmentation stage and then the tracking. Now, for real applications, image processing does not end with formal results, it is followed by some decision, triggering actions. Thus it is necessary to decide between working harder on processings than on the decision stage or opposite ("process before or after"). When decision appears as mere thresholding, such simplicity results most often from the complexity of the previous processing that have pointed out a set of pertinent features. But decision may be as complex to make as in segmentation algorithms, when one merges regions thanks to a set of criteria and to a sophisticated relaxation process. Facing our problem, what will be the choice? The astrophysicists' knowledge is not sufficient enough to decide, without any ambiguity, on the exact position of a filament (or facula) border (and that is another reason why the motion has always been studied through the sunspots). Hence, one would better process to the best possible accuracy, and then, decide in the simplest possible way. We must organize all known features connected to the structures to be extracted, in such a way that processing remains trackable. As for the motion stage, the astrophysicists have extracted the theorical rotation law and they have set out some properties to constraint the motion of both structures. In such a case some strong prediction based tracking will lead to an easy verification stage.

3 FROM PROPERTIES TO ALGORITHMS

3.1 Extracting the pertinent features

The knowledge stemmed from the study of the sun (on the side of the astrophysicists) leads us to the primary graph of *figure 5*. Though it appears quite simple, it enables to extract a set of properties not necessarily observable to the naked eyes. In this network we introduce entities (as filaments and faculas) and their properties (put between brackets). As in every hierarchical network, entities inherit the properties of their parents. When progressing along the network, the properties become sharper and sharper and refer to less and less entities: the knowledge organizes the processes to be performed and thus saves computation time.

We aim at extracting both faculas and filaments so, the Hα radiation is to be processed as both structures can be found in its images. The global property that matches all the so called pertinent areas is the **variable** nature of their emissivity (or absorption) in respect with the homogeneous nature of the solar background.To a certain extent, both following descriptions are admissible:

In a filament or a facula, the amounts of matter respectively concentrated at adjacent points

are very different.[merely because radiations cross more or less matter]
In a filament or a facula, neighbours of a pixel have totally different luminances.

As filaments (respectively faculas) are much more absorbent (respectively emissiv) than the background representating variability in terms of variance is not relevant as this formulation is more dedicated to the border extraction than to the extraction of the structure itself. This leads to make use of textural description of the phenomenon. In [4], Lowitz describes the efficiency of an histogram norm for pre-segmentation steps. Results obtained through this method were acceptable with an automatic threshold performed from the histogram norm. But another textural clue leads to the same results with much less computation. As the magnetic field tubes are about 1 pixel wide, and they push the chromosphere's matter more or less but accordingly, an even simpler way of pointing out the luminosity variability of pertinent areas is merely to count the number N of adjacent pixels P[i] of P[k] whose luminance L(i) is contained between $L(k) - \sigma_0$ and $L(k)+ \sigma_0$ where σ_0 is the standard deviation of the solar background. Then P[k] will be a part of a pertinent area if this number N is smaller than N_0 (N_0 is computerized from cumulated histogramm of every results).

As we are using neighbourhoods, their size is to be determined. Let us first define the upper limit of this size. As it is visible in *figures A3 and A4*, there are some ramifications (called the "feet" in the case of filaments).

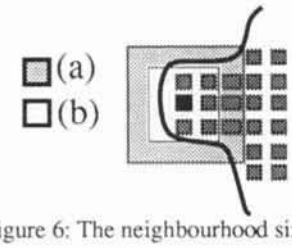

figure 6: The neighbourhood size

"Sufficient accuracy" means extracting these small details. Figure 6 shows trivialy that when the neighbourhood size is smaller than the details the result is correct (refer for instance to mathematical morphology). That gives us the upper limit. The spatial variation of the matter density gives us the low limit (non homogeneous must be understood as a macroscopical description). We have chosen a size value of $9*9$.

Once pixels included in both filament and facula classes have been isolated (let be this image I_{zone}) they remain to be separated, using the luminance criterion. As the sun is a spherical light source, this criterion is operated coronas after coronas (with width of 10 pixels) to take into account the luminance decrease from center to border. That can be formalized by:

$$L[k] \leq S(r) \pm \alpha.\sigma(r)$$
$$\Rightarrow P[k] \in \{\text{Filaments or Faculas}\}$$

That gives us I_{dark} and I_{bright}. Shape and location criteria are dedicated to regions (and we just get a set of pixels); before processing them, a logical "AND" is computed between I_{dark} and I_{zone} to obtain I_{fil} (respectively I_{fac}).

These images are then labelled to get regions. First of all, the regions whose surface is less than 10 pixels,are eliminated. Indeed, even if they refer to filaments or faculas they are so unstable because they are small, that they cannot be tracked and very likely they will be false alarms.

The shape criterion is bound to the location criterion as follows:

a filament located near the equator is really threadlike and is brought into alignment with meridians.
a filament located near the poles is quite round and to some extent brought into alignment with parallels.

To classify these two kinds of filaments we use the inertial matrix:

$M_I = \begin{pmatrix} I_{xx} & -I_{xy} \\ -I_{xy} & I_{yy} \end{pmatrix}$ where, for an example $I_{xy} = \sum_{surface} xy$.

This matrix can be put into a diagonal form in the principal inertial frame and the rotation angle provides us with the pattern orientation.Let us illustrate this.

- First case $M = \begin{pmatrix} 35.64 & -74.8 \\ -74.8 & 1054.97 \end{pmatrix}$
- Second case $M = \begin{pmatrix} 110.67 & -35.36 \\ -35.36 & 46.71 \end{pmatrix}$
- Third case $M = \begin{pmatrix} 76.23 & -76.23 \\ -76.23 & 76.23 \end{pmatrix}$

In the first case the diagonal matrix is equal to: $I_{diag} = \begin{pmatrix} 1064.43 & 0.0 \\ 0.0 & 30.18 \end{pmatrix}$

Hence the principal direction is: $\alpha = 94°$ and the ratio between eigenvalues is: $\rho = 35$

In the second case the results lead to: $\alpha = 156°$ and $\rho = 4$

In the third case, that is a representation of a false alarm we notice that:

$\alpha = 135°$ and $\rho = \infty$

So, if the first form is located near the equator, then it can be a filament whereas the third form can be neither a filament nor a facula. There is a case that demands another parameter. It appears sometimes that near the regions of strong magnetic field, filaments are folded over.Thus the inertial moments are approximately equal. As it happens only near the equator, the number T which is the ratio between the including box surface and the filament surface is convenient. If this ratio is small, then it cannot be a false alarm when located near the equator. The extraction results have really satisfied the astrophysicists, who have come to understand that some details revealed by detection could even suggest a local magnetic field topography. As it is shown *figure A3* after extraction of the filament seen in *figure A2*, the feet have been exhibited and since these feet are constituted of plasma that flows along the magnetical tubes, it is possible to get the orientation of the magnetic field near the filament (they behave as true tracers).

Interesting enough, it has been possible to design every algorithms, from varialibility detection to false alarms elimination without a single look to the images, and the results just prove the reliability of such a procedural method.

After these processes, images are segmented into labelled regions, and tracking can begin.

4 TRACKING THE FILAMENTS

4.1 The matching scheme

Having at hand all the filaments, described with their skeletons, there remains to track them along images. We have chosen this kind of description because of the physical knowledge of their evolution. As we saw it in the second part, filaments are quite unstable regions of the surface. The head and tail of a filament can disappear from an image

to the other, just because the magnetic field that was supporting it collapses, or more often because the plasma just spreads about. The same phenomenon occurs with the borders of the filaments and thus it appears releavant to describe them using their medial axis line.

To track the filaments, we use a general prediction/verification scheme. We know the theorical rotation law of the surface, so it is easy to predict the motion of a region. That means that we will only extract the deviation from the standard rotation law. As we want a straigthforward verification (that means a simple decision stage) we will have to work the best on the prediction.

As we saw it in the first part, the motion on the sun surface is latitude dependent. Thus, a filament can be twisted and its movement cannot be reduced to a composition of rotation/translation. This does not enable us to use Freeman's code that is not an invariant representation for this kind of motion. Despite this, as we know the theorical motion law, the use of points coordinates enables a simple pre-computation of the motion.

As filaments are described in terms of monodimensionnal structures, it is convenient and very powerful to use elastic matching as in word recognition [6,7].

A region is described as a set of points $P_i[X,Y]$. The aim of the elastic matching is to calculate the best local motion that will transform R(t) into R(t+1). This can also tell us which is the best association between several candidates. Then, by using variable undersampling of the sets of points, it is possible to shift from pattern matching to "point to point association".

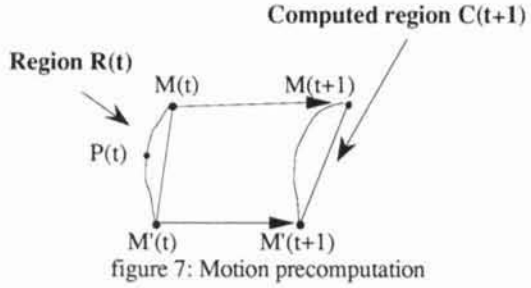

figure 7: Motion precomputation

We first have to compute the distance between every points of associated regions (let us call them R(t) and R(t+1)). Let P(t) be a point of R(t), and let (M,M')(t) 2 antagonistic neighbours of P(t).(*see figure 8*)

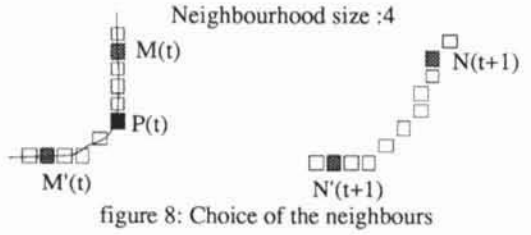

figure 8: Choice of the neighbours

Selecting a couple of points, we calculate the new position using the theorical law. Thus from a couple (M,M')(t) of region R(t) we compute the position of the couple (M,M')(t+1) (*see figure 7*). This couple of points is compared with every couples (N,N')(t+1) of R(t+1) (*see figure 9*) (distance between N and N' is equal to distance between M and M' as we know that motion doest not involve any homothety). On the basis of matching points M'(t+1) and N'(t+1), the deviation d(i,j) between the theory and what is observed, is given by the L_2 norm of $\vec{u}$. That norm would be correct for isotropic moves. But, following physics again, the motion is principaly due to the rotation along the North to South axis. The "meridian deviation" (as called by the astrophysicists) is less than 10% of the global motion. So we can constrain computations of the $\vec{u}$ norm following the equation:

$$d(i,j) = \sqrt{(x_{M(t+1)} - x_{N(t+1)})^2 + K.(y_{M(t+1)} - y_{N(t+1)})^2}$$

where $K \geq 1$.

This will prevent too strong deformations along the Y axis from being taken into account (the cost of Y moves is $\sqrt{K}$ greater than the cost of X moves).

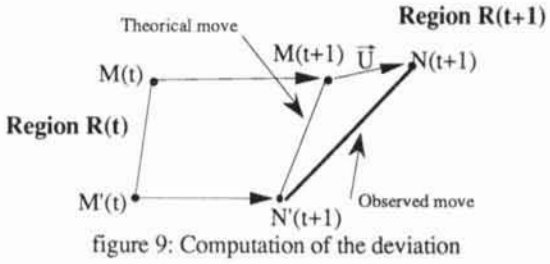

figure 9: Computation of the deviation

In case of a defect free movement, we have of course $\vec{u} = \vec{U}$. The dynamic equation used is symetrical in accordance with the physical knowledge that enables both streching and contraction. The local equation used to compute the local cost g(i,j) is:

$$g(i,j)=\min\begin{Bmatrix} g(i-2,j-1)+d(i-1,j)+d(i,j) \\ g(i-1,j-1)+d(i,j) \\ g(i-1,j-2)+d(i,j-1)+d(i,j) \end{Bmatrix}$$

so that the local cost g(i,j) is computed for 3 different ways, the diagonal one (that is defect free) and 2 symetrical ways that perform contraction and streching.

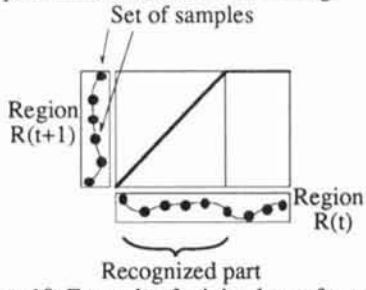

figure 10: Example of minimal transformation

All this is quite similar to "dynamic time warping" in speech processing. Some variation comes with multi-resolution.

4.2 From region matching to point matching

Variable undersampling of the data points has two aims. First it saves computation time. Second, and that is the major point, if we compare several associations as the undersampling reduces, we do not have to compare directly the costs to one another, we just have to work separately on the costs evolution using no global threshold. As it is shown in *figure 11* and more precisely in *figures A9 and A10*, the cost srongly diverges when trying to match dissimilar regions.

Rules, for match guiding are described bellow:

- *if there is only one possible matching ($R \rightarrow R'$) increment the set of sampling points to the maximum value (neighbourhood size of 1) and perform point to point matching. Verify the prediction.*
- *if there are many candidate regions increment*

the set of sampling points to the next value and store the costs. If an association reveals some discontinuity in the cost variation reject it and keep on proccessing the others. Verify the prediction of the remaining associations.

In order to verify an association, we compute the α and β coefficients of the rotation law (*see figure 1*)that match best (using standard quadradic minimization) the association and we verify that they stay in range of the theorical ones.

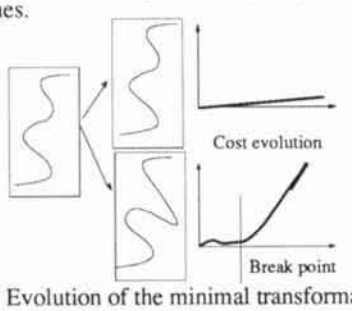

figure 11: Evolution of the minimal transformation cost with the set of samples

This kind of tracking scheme is interresting because it allows to perform global matching between regions and also space scaled associations which accuracy depends on the segmentation stage resolution. It works on symbolic features inlike the optical flow (there is no constraint on the evolution of the luminance) but of course needs a pre-segmentation stage and above all some a priori knowledge on motion. The use of the deviation vector $\vec{u}$ is very convenient to apply anisotropic motion constraints

5 RESULTS

5.1 Segmentation

The segmentation needs at least the 2 parameters: dark and brigth threshold coefficients. The raw data are 512x512 1 byte images. We first calculate "spherical mean image" and "non homogeneous" index. These images will be used for detecting both filaments and faculas. We compute for every pixels the answer to the different criteria and we label the obtained image. On each region we perform false alarms elimination using the rules described in section 3. Finally we compute the skeleton of every regions.

Figure A1 shows the raw image of the sun surface of June the 2nd 1982, as it comes out of the spectroheliograph.

Figures A2 to A4 give examples of both detections before the elimination of false alarms. One can observe the "feet" of the filament that recall exactly the local topography of the magnetic field. In a certain extent, that may help astrophysicists to predict solar erruptions as magnetic field distorsions.

5.2 Tracking

Figures A5 and A6 give an idea of the cost evolution while trying to match different edges. Edge S(t) is to be matched with edge S1(t+1) and with S2(t+1). S2(t+1) is very similar to S(t) while S1(t+1) has been added strong distorsions. One sees that the cost diverges very quickly when trying to match S1(t+1).

Figure A7 represents the experimental rotation law (we just added extrem latitude points to extend the curve). This curve, processed with 30 images (extract from June 1982 data base), has the same statistic weight as those obtained by the astrophysicists in 6 months, thanks to the results of elastic matching.

One can also observe that the north hemisphere is more "differential" than the south hemisphere. This has been confirmed by recent works that point out the existence of a longitudinal roll in the north hemisphere.

We have also extracted some "strange filaments" that present strong distorsions highly visible with the elastic matching. Those filaments are moving much faster than expected.They also disapear from the sun surface within a few days. Very recently,, American reseachers have found that when a filament disapears, it litteraly "surfs" the magnetic tubes that were sustaining it, thus moving much faster than the surface.

5.3 Accuracy

The solar radius in the 512x512 images is 222 pixels long. We estimate a maximum error of 1 pixel to locate the skeleton. It leads to a 2 pixels error when computing the distance. Inverting the orthogonal projection, we obtain:

$$\delta\theta = \frac{\delta x}{r.\cos\theta} \Rightarrow \delta\theta = \frac{1}{111.\cos\theta} \quad \text{knowing that: } \Omega = \frac{d\theta}{dt}$$

$$\Rightarrow \frac{d\Omega}{\Omega} = \frac{2\delta\theta}{\Delta\theta} + \frac{2\delta t}{\Delta t}$$

we can neglect \F(2δt;Δt) in the above sum and then:

$$\frac{d\Omega}{\Omega} = \frac{1}{111.\Delta\theta.\cos\theta}$$

When limiting the scan in θ from -80° to 80° we obtain the upper limit of the error:

$$\frac{d\Omega}{\Omega} \leq 0{,}4\%$$

that is well within the range of the accuracy obtained by astrophysicists.

6 Conclusion

The claim for originality in this paper is twofold. First, the application is not common. Due to the image formation process, very interesting choices between texture, edges, motion operators occured. They allowed to check some enjoyable image processing expertise according to the methodology in our laboratory [8]. Second, to make the whole process fully automatic, the knowledge about physical phenomena had to be embedded into a semantic network, leading to rules which are sort of a rough expert system in the application, triggering itself a prediction/verification scheme any time it is necessary. More precisely we have stressed upon how physical properties of an observed object can help a lot towards designing its detection. It has pointed out the pertinent properties that were to be extracted in the image and it has given the natural linking for processings. The accuracy of the extraction has convinced the astrophysiscists to rely on image processing, and it has confirmed us in the pertinence of such a methodology. It is to be noticed that an automatic real time solar surveillance system is going to be installed, in cooperation with our laboratory.

As for the tracking scheme it is derived again from physical observations of the surface evolution. The theorical rotation law has been helpful to predict motion but the results have prompted astrophysicists to have doubts on its validity. Image processing has enabled them to analyze new results and has given a greater number of motion measurements. This will probably lead to a new model of rotation and will circle the cooperation between physics and image processing.

We are now working on a spatial tracking, using the three radiations, in order to extract the 3D evolution of both structures, second we have worked on automatizing the whole process thanks to a computer implementation of the rules quoted above and to their link with the Image Processing procedures.

7 Bibliography

[1] Howard, R. & Labonte, B.J. (1980). *The sun is observed to be a torsionnal oscillator with a period of eleven years.* Ap J. 239:L33-L36

[2]Ribes, E. & al (1985). A large scale meridional circulation in the convective zone. Nature, n°318, 170-171

[3] Chetverikov, D. (November 14-17 1988). Experiments in the rotatio-invariant texture discrimination using anisotropic feature. 9th ICPR, Vol 1, 61-63

[4] Lowitz, G.E. (1983). Can a local histogram really map texture information? Pattern Recognition, Vol. 16, n°2, 141-147

[5] Weska, J.S., Dyer, C.R., Rosenfeld, A. (April 1976). A comparativ study of texture measures for terrain classification. Systems, Man and Cybernetics IEEE Trans., Vol SMC VI, n°4, 269-285

[6] P. Adam, B. Burg, B. Zavidovique. (8-11 April 1985). Dynamic programing for region based patter recognition. ICASSP/IEEE - ASJ Tokyo.

[7]B. Burg, Ph. Missakian, B. Zavidovique.(June 1987) Reconnaissance de silhouète par programmation dynamique. 2nd Int. Conference on Computers and Applications. Beijing, China.

[8] B. Zavidovique, V. Serfaty, C. Fortunel. Mechanism to capture and communicate image-processing expertise. IEEE Software Nov. 1991. P 37-50.